Determining the Properties of the NGC 7789 Open Cluster from Colour-Magnitude Diagrams

Lewis Woods

22 December 2023

ABSTRACT

The available methods for determining the properties of main-sequence and evolved stars are few. The most ubiquitous techniques are dependent on stellar physics models which incorporate mechanisms that are not fully understood, leading to inaccuracies in model-dependent measurements. In this study, photometric analysis of the NGC 7789 open cluster was carried out. Numerous evaluations of age, distance and reddening exist for this cluster but almost exclusively by a single method of isochrone fitting. This method was applied here to measure an age of 1.5Gyr and E(B-V) = 0.30, both of which are consistent with existing literature. The distance measurement of 1800pc was consistent with other isochrone-fitting studies but was found to be notably less than the results from parallax measurement. This disparity highlights the need for improved models of stellar physics to enhance the reliability of model-dependent methods and the measurements gained from them.

1 INTRODUCTION

The available methods for determining stellar ages are varied (see Soderblom (2010)). For main-sequence stars, there are three key techniques, two are model-dependent and the third is empirical. The empirical method described in Barnes (2007) is known as *gyrochronology* and can be used to estimate the age of an individual star to within 15% through measurements of colour and rotation period. The most recent of the model-dependent methods, *asteroseismology*, can be applied to individual pulsing stars – which are observed at most phases of the Hertzsprung-Russell (HR) diagram. It utilises observations of the oscillation modes of these stars by comparing them to models of stellar physics to determine the age of the star, as summarised by Lebreton & Montalbán (2008). The final method, termed *isochrone-fitting*, is the oldest and is most often applied to large coeval ensembles of stars (see Brogaard et al. (2017); Dinescu et al. (1995); Olsen et al. (1998) for examples) but can also be applied to individual stars through a Bayesian statistical approach as in Jørgensen, B. R. & Lindegren, L. (2005).

This method of fitting isochrones to large coeval populations was applied in this project to the NGC 7789 open cluster (OC). OCs are of great astronomical interest as they are useful for studying stellar evolution models since all stars in an OC were initially identical in chemical composition. Thus any observed differences in the present state of their atmospheres are dependent on processes of stellar evolution. Additionally, because all stars have the same age, distance and metallicity, their physical properties, such as effective temperature, are easier to determine than for field stars.

Specifically for isochrone models, an OC like NGC 7789 acts as an excellent test of their validity. The first colour-magnitude diagram (CMD) of NGC 7789 by Burbidge & Sandage (1958) revealed a 'red clump' of core He-burning stars, a significant number of blue straggler stars, and a main sequence with a pronounced turnoff towards a clear red giant branch (RGB). Such well-defined regions corresponding to the different phases of stellar lifetimes make NGC 7789 very useful for modelling stellar evolution.

This report details the determination of the age, distance and reddening of NGC 7789 via a process of V and B-band photometry, the observational data of which was used to produce a CMD and find a best-fitting isochrone. The Planning section will delineate the suitability of NGC 7789 as a target for this project. The data taken will be covered in the Observations section and the steps taken to calibrate and analyse the CCD images will be described in the Analysis section.

Quantity	Value	Unit
CCD Readout Noise (RMS)	10	e^-
CCD Dark current at 0°C	0.5	e^-/pixel/second
CCD Quantum Efficiency (V band)	85%	–
Telescope Aperture Diameter	0.406	metres
Sky Background (V band)	21.5	magnitudes
Source Brightness (V band)	13	magnitudes

Table 1. Summary of key information used to predict the SNR in data from NGC 7789.

2 PLANNING

2.1 Signal-to-Noise Ratio

The signal-to-noise ratio (SNR) is defined in Equation 1,

$$SNR = \frac{S_0}{N} = \frac{S_0}{\sqrt{S_0 + S_s + S_d + R^2}} \tag{1}$$

where N is the total noise which is given by the standard deviation of the total signal. S_0, S_s, S_d and R represent the components of the total signal from the target, sky background, dark current and readout noise respectively.

Using the specifications of the Hicks telescope and the CCD model (see key information given in Table 1), the number of photoelectrons from each of the above components can be estimated.

For a 300s exposure using the V band filter, the SNR was predicted to be 783, an excellent ratio which allows for very precise photometry at the main sequence turnoff of NGC 7789. The SNR considerations for target selection are covered in greater detail in the next subsection.

© 2023 The Authors

2.2 Target Selection

Any potential target had to satisfy the following conditions (all of which are described in more detail below):

- Old enough to have main-sequence turnoff and RGB.
- Bright enough to give a good signal-to-noise ratio.
- Visible in the night sky from Sheffield in October and November.
- Small enough in angular size to fit within the field of view of the Hicks telescope.

Several open clusters were identified as potential targets for this study, these were NGC 7789, NGC 6939, M67, and NGC 2627. The latter two were rejected due to their unobservable position in the sky from Sheffield during October and November.

In order for the method of isochrone-fitting to be applicable, the target cluster must be of at least intermediate age so that a significant number of stars have turned off the main sequence and evolved into red giants. Both NGC 7789 and NGC 6939 satisfy this constraint.

Additionally, the target's suitability for the observatory must be considered. The target must be bright enough to produce an adequate SNR given the specifications of the equipment in use. Grouping the parameters S_0, S_d and R^2 into one variable Ω, the number of photons from the target can be related to the SNR via Equation 2.

$$S_0 = \frac{1}{2}(SNR)^2\sqrt{1+\frac{4\Omega}{(SNR)^2}} \tag{2}$$

For precise photometry, it is sensible to require an SNR of 100 or greater. Setting this as the minimum for a suitable target, S_0 can be found from Equation 2. Converting this value into flux, the minimum brightness required to satisfy this condition is given by Equation 3.

$$m_0 = -\frac{\log\left(\frac{F_T}{F_V}\right)}{0.4} \tag{3}$$

Where m_0 and F_0 are the apparent magnitude and flux of the target respectively, and F_V is the flux of Vega.

All in all, requiring an SNR of at least 100 implies that any appropriate target star must have a magnitude m_0 of ~ 15.5 or brighter. Since NGC 7789 and NGC 6939 both have a typical V-band apparent magnitude of ~ 13 at the main-sequence turnoff, they are both bright enough to serve as the target for this project.

Further to this, the target needed to be visible from Sheffield at night during the months of October and November. To determine whether NGC 7789 would be visible during this time, the Right Ascension (RA) and Declination (Dec) were calculated. For the night of October 9th 2023, the RA of the Sun was calculated as 13h 12m, meaning the local sidereal time was 1h 12m. At midnight, the local sidereal time represents the RA of an object as far away as possible from the Sun on the sky (which would be an ideal target for observation). The best possible Declination for a target is directly overhead. Thus, an ideal Declination can be obtained directly from the latitude coordinate of the observatory. In the case of the Hicks observatory, this is 53d 22m 51.6s N. Using sky chart software, the coordinates of NGC 7789 at this time were RA = 23h 57m and Dec = 56d 42m. The coordinates of NGC 6939 were RA = 20h 31m and Dec = 60d 39m. These coordinates are close to those calculated for an ideal target, once again making both NGC 7789 and NGC 6939 suitable clusters to observe.

The final consideration is the angular size of the cluster. With a 0.67x focal reducer, the Hicks telescope has a field of view of 18' 49" arcminutes by 12' 38" arcminutes. The angular size of NGC 7789 is ~ 16′, while that of NGC 6939 is ~ 7′ so the Hicks telescope is sufficient for observing the whole of the latter and the bulk of the former.

Frame Type	Exposure Time (s)	Filter	Number Taken
Light	30.0	B	3
Light	300.0	B	3
Light	30.0	V	3
Light	300.0	V	3
Flat Field	7.0	B	3
Flat Field	4.0	V	3
Dark	30.0	–	3
Dark	300.0	–	3
Bias	0.0	–	3

Table 2. Summary of all exposures taken during observation.

In the end, the more populous cluster (NGC 7789) was chosen as this would allow for a much larger data sample, resulting in a greater number of data points on the CMD and therefore making the method of isochrone fitting more appropriate.

3 OBSERVATIONS

There were a total of 12 exposures taken of the NGC7789 cluster - 3 for each combination of filter and exposure. In addition, a total of 15 frames were taken to measure the flat field, dark current, and bias voltage of the CCD. Table 2 offers a summary of every exposure taken during observation.

The flat field frames were obtained by placing a uniform light source over the telescope aperture and taking 3 short exposures for each filter.

The dark frames were taken by closing the shutter on the telescope and taking 3 30s exposures and 3 300s exposures.

The frames representing the bias voltage were acquired by taking 3 0.0s exposures.

Processed images of all 3 of these measurements can be seen in Figures 1, 2 and 3.

Noteworthy weather conditions on the night of the observation (Nov 6th 2023) are as follows:

- The moon had not risen.
- It was a grey night.
- Scintillation observed in stars indicated highly variable seeing.
- Presence of thin high cloud.
- Some lower clouds observed.
- 7mph winds.
- 85% humidity.
- Temperature was 8°C.

4 ANALYSIS

4.1 Calibration

Converting the raw CCD images into usable data involves calibrating the images by subtracting dark current and bias voltage, and normalising for the flat field of the telescope. This was done by creating master frames that could be used to correct for the various forms of noise in the raw images.

For the bias voltage, a master frame was created by taking the mean of the three bias frames (to reduce the effect of readout noise on the measurements for bias voltage). The master bias is shown in Figure 1.

Two master dark frames were created to account for the dark current in each exposure time (30s & 300s). These frames were made by

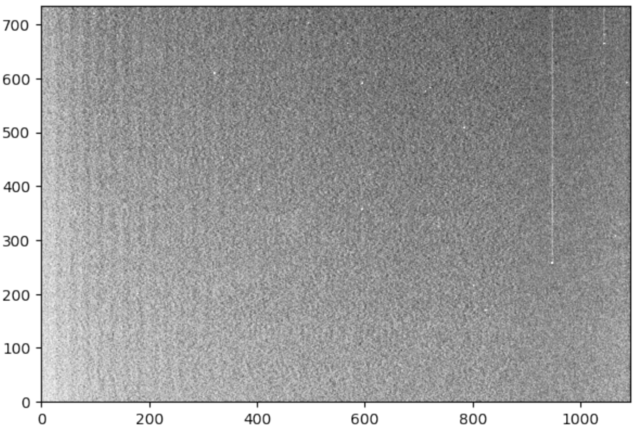

Figure 1. The master bias frame created by averaging the 3 bias frames.

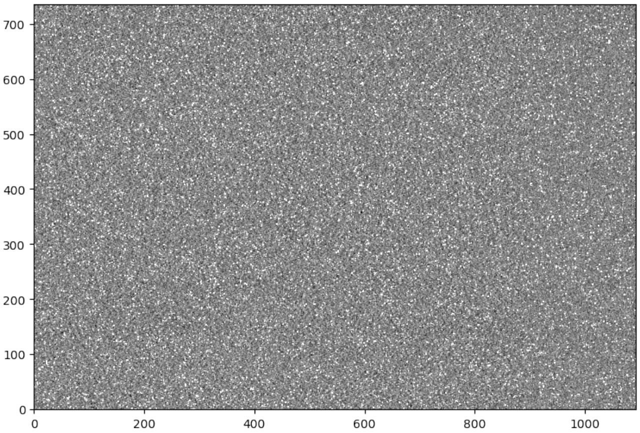

Figure 2. The master dark frame for the 300s exposure time.

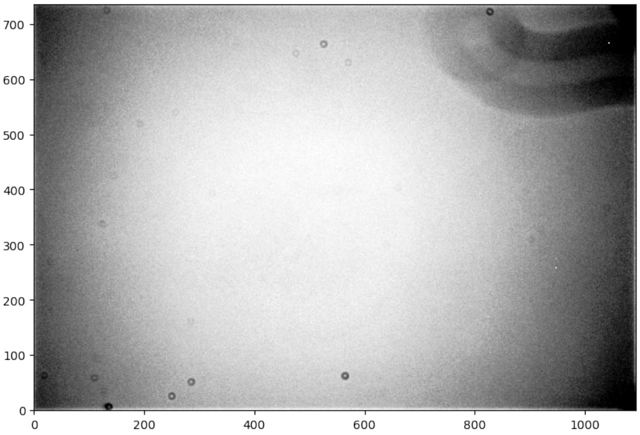

Figure 3. The master flat created for the V band filter.

subtracting the master bias from all dark frames and then taking the median of the three in each exposure time. The master dark frame is shown in Figure 2.

To correct for the flat field, after subtracting the bias level, the mean was taken for the three frames for each filter, then the resulting averages were normalised to give the master flat field in each band (V & B). The master flat field is shown in Figure 3.

The raw images were then calibrated by subtracting the bias level across all images. Subtracting the dark current for the correct exposure time, and then dividing by the flat field for the correct filter.

Finally, the images were aligned and averaged into one frame for each combination of exposure time and filter. The resulting calibration is shown next to its raw data for the 300s exposure V band image in Figure 4.

4.2 Absolute Photometry

The next stage of analysis was to determine calibrated magnitudes of the stars in the CCD images. First, a detection algorithm was used to extract data from any sources with a FWHM of approximately 4" with minimum brightness 4 times greater than the standard deviation of the background. The figure of 4" was obtained from the FWHM shown in Figure 5 using the conversion of 1.04" per pixel as per telescope specifications.

Aperture photometry was then carried out on the detected stars to calculate *instrumental* magnitudes using the following settings:

- Aperture Radius = 4 pixels
- Inner Sky Annulus = 10 pixels
- Outer Sky Annulus = 20 pixels

The data of the detected sources is shown against the CCD image used in Figure 6.

The APASS catalogue was then used to match many of the detected stars to those in the catalogue and determine their *calibrated* magnitudes. The offset between the calibrated and instrumental magnitudes is the zeropoint for the observations. This was calculated by taking the median difference between the two sets of magnitudes. The calibrated magnitudes for all the stars in the data were then calculated by adding the zeropoint to the instrumental magnitudes. However, it was necessary first to ensure there were no saturated stars in the data. Figure 7 shows evidence of saturation in the 300s exposure time for stars brighter than approximately 12.5 magnitudes. It can also be seen from the data in Figure 8 that these same stars show little to no saturation in the 30s exposure.

To correct this, the zero point was calculated for both exposure times and the instrumental magnitudes were converted into calibrated magnitudes. Then the saturated stars in the 300s dataset were replaced with their counterparts in the 30s dataset. The resulting data is shown in Figure 9. This process was repeated for the B band data to give two datasets containing as little saturation as possible.

To ensure there were no unreliable data points, any points where the RA and Dec coordinates did not match up in the B band and V band to within a 2-dimensional distance of 3 arcseconds were removed from the data.

The CMD was then plotted using the errors on the instrumental magnitudes (calculated by the algorithm that matched the data points to the APASS catalogue) and propagating them for (B-V). Figure 10 shows this CMD in which the main sequence, red clump and RGB are visible. Due to the errors in this CMD the data for about half of the main sequence is not suitable for fitting. Thus, when producing isochrone fits for the CMD, the main sequence turnoff and the red clump were used as reference points for fitting by eye.

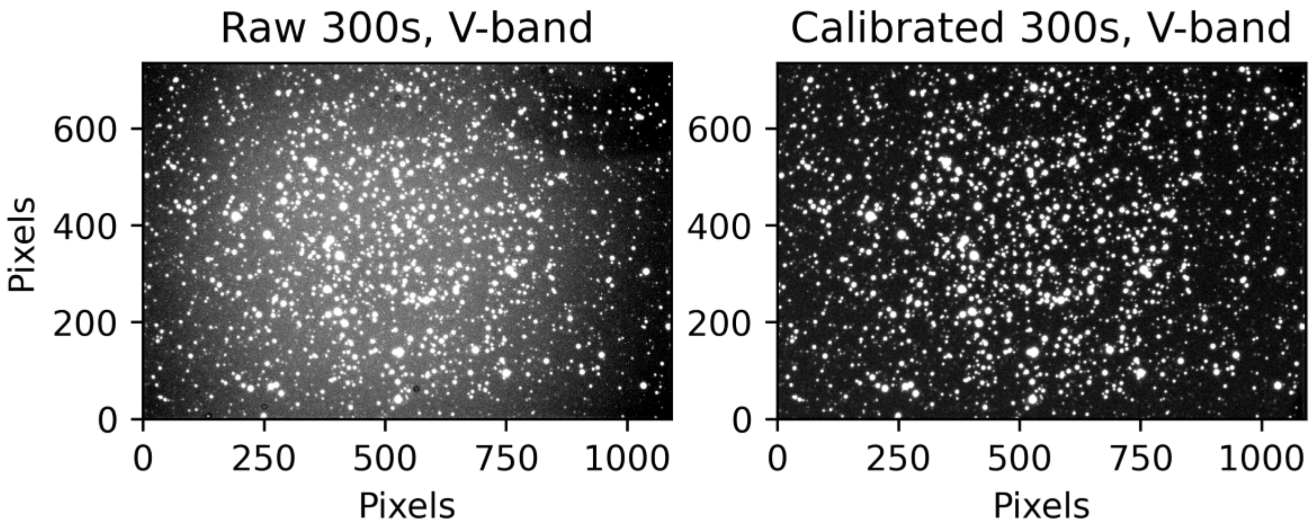

Figure 4. One raw CCD image in the V band with 300s exposure time is shown next to the average of the 3 corresponding CCD images corrected for bias level, dark current and flat field.

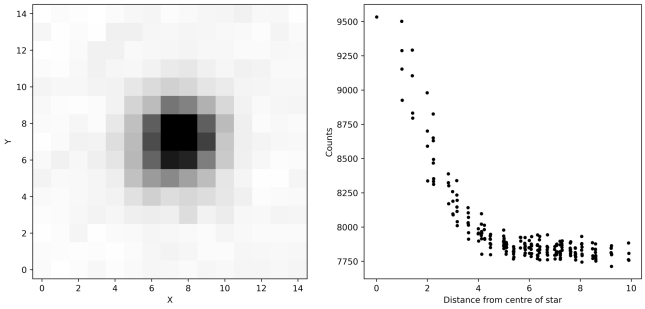

Figure 5. The Full-Width Half Maximum of a detected star is approximately 2 pixels which corresponds to 4 arcseconds.

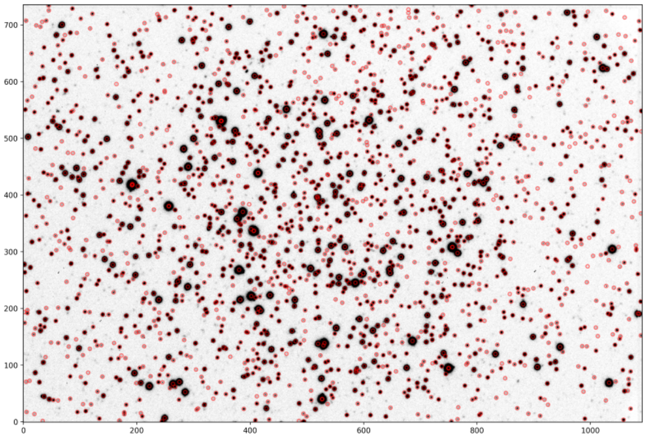

Figure 6. The detected sources are shown by the red circles on top of the CCD image.

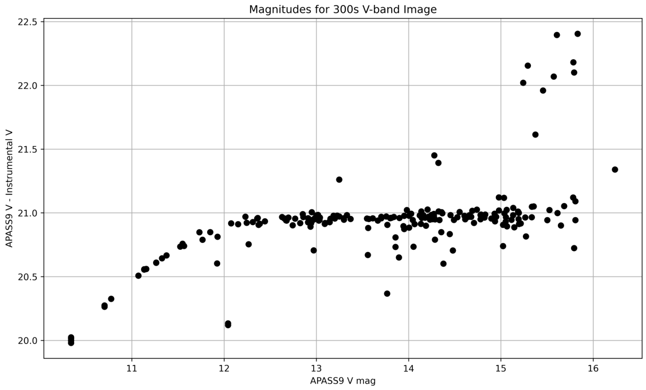

Figure 7. Plot of the difference between calibrated and instrumental magnitudes against calibrated magnitudes for the **300s** exposure in the V band. Saturation can be inferred from the tail-off below 12.5 magnitudes.

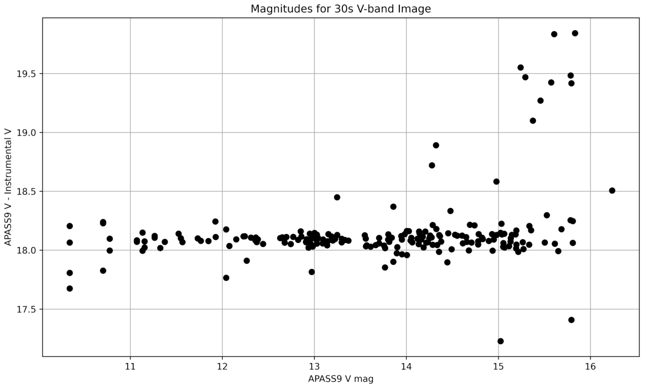

Figure 8. Plot of the difference between calibrated and instrumental magnitudes against calibrated magnitudes for the **30s** exposure in the V band. Far less saturation is observed in the data.

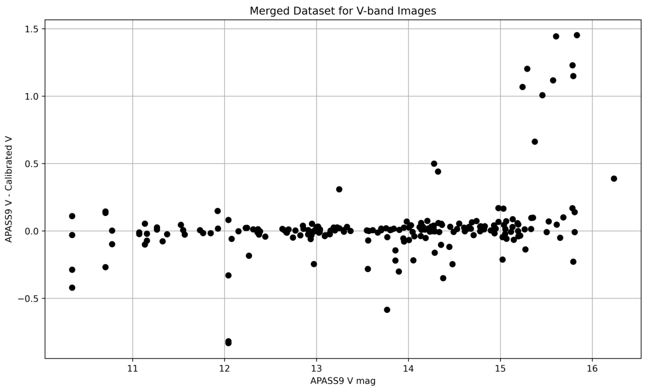

Figure 9. Plot of the difference between the *catalogue* calibrated magnitude and the *calculated* calibrated magnitude against catalogue calibrated magnitude for the merged dataset. Notice the horizontal distribution centred on a magnitude of 0.0 which is expected from such a plot.

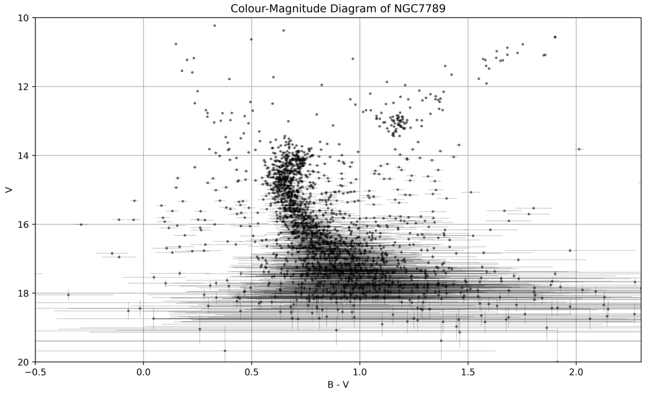

Figure 10. Colour-magnitude diagram for NGC7789 showing the main sequence and red clump. Dimmer stars can be seen to have substantial errors compared to brighter stars.

4.3 Isochrone Fitting

The isochrones used to fit the CMD were the MIST models from Choi et al. (2016). The isochrone for a given age is imported and adjusted for extinction A_v, reddening $E(B-V)$, and distance d, to line it up with the apparent magnitudes in the data obtained for NGC7789. The initial values used for these parameters were:

- $E(B-V) = 0.25$mag Bartašiutė & Tautvaišienė (2004)
- $A_v = 3.1E(B-V) = 0.775$mag Schultz & Wiemer (1975)
- $d = 2754$pc Gim et al. (1998)
- Age = 1.7Gyr Gim et al. (1998)

This produced an isochrone that was close to the data but was necessary to correct.

5 RESULTS

The best-fitting isochrone was found by adjusting the parameters of age, distance and extinction from the initial fit so that the isochrone lined up with the main-sequence turnoff and the red clump as well as possible. The parameters found for the best fit were age = 1.5Gyr, distance = 1800pc, and extinction = 0.92mag. From here, upper and lower fits were found by changing the age parameter and then adjusting the distance and extinction to realign the new fit with the best fit. This was repeated, each time taking a greater difference in the age until the three parameters could no longer be combined in any way to produce an acceptable fit. In this way, the upper and lower fits were used to determine the uncertainties on each parameter. All 3 fits can be seen plotted together on the CMD in Figure 11 with a legend that displays the parameters used for each.

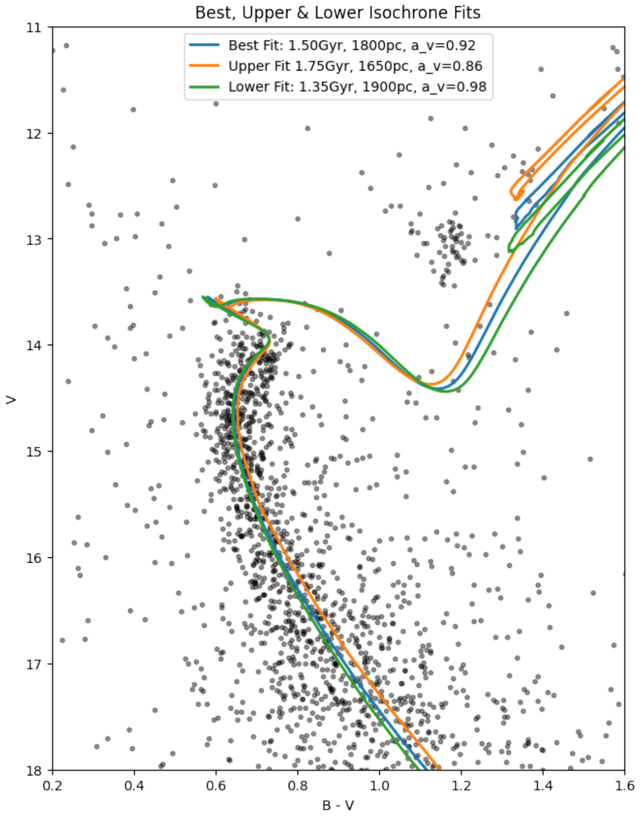

Figure 11. The best, upper and lower fits are shown. Each one aligns well with the main-sequence turnoff and gives a reasonable fit to the red clump.

From Figure 11, the results of this observation can be drawn. The age of NGC 7789 was determined to lie in the range of 1.35–1.75Gyr with a best fit of 1.50Gyr.

The distance to the cluster lies between 1650 and 1900pc with a best fit of 1800pc.

The extinction is between 0.86 and 0.98 magnitudes with a best fit of 0.92 magnitudes. Finally, the relation between extinction and reddening can be utilised once more to obtain a value for the reddening of $E(B-V) = \frac{A_v}{3.1} = 0.30$, with an uncertainty range of 0.28 to 0.32.

6 DISCUSSION

As was presented in the Planning section, NGC 7789 was chosen for this project as its brightness allows for precise photometry at the main-sequence turnoff. Data on stars in this region and the brighter red clump and blue straggler regions can be seen to have minimal uncertainties in Figure 10. Despite this, there are still sources of systematic error. Small divergences of the filters used from the Johnson-Cousins system and higher-order extinction terms would have a minor effect. The dominant sources of systematic error are

saturation and inaccuracies in the zeropoint calculations.
Saturation affects the brightest stars in the sample and although efforts were taken to remove saturation from the data (see Figure 9) it could not be removed absolutely and saturation is still visible (albeit to a lesser degree) in the brightest stars in the corrected data.
Furthermore, in the plots of the data from which the zeropoint was calculated, it can be seen that a number of the dimmer data points are instrumentally less bright than should be expected from the catalogued magnitudes. This wouldn't affect the median offset but does hint at imprecision in the data, possibly due to less-than-ideal weather conditions during observation.
The result of 1.5Gyr obtained for the age of NGC 7789 compares well with the existing evaluations:

- 1.1Gyr Mazzei & Pigatto (1988)
- 1.2Gyr Martinez Roger et al. (1994)
- 1.7Gyr Gim et al. (1998)
- 1.4Gyr Vallenari et al. (1999)

Taking the uncertainty in the age to be half the range (0.2Gyr), means this result is within one σ of the two most recent evaluations. Unfortunately, no age measurements of NGC 7789 using other methods are available so comparisons to different techniques are not possible.
As for the measurement of the distance to NGC 7789, the best fit of 1800pc compares very well with the value of 1840pc obtained via isochrone fitting by Bartašiutė & Tautvaišienė (2004). However, the result of 2067pc obtained by Gao (2018) using parallaxes with the Gaia satellite agrees less well. Once again taking the uncertainty as half the range, which for the distance measurement is 125pc, then this result is just outside the 2σ range. This discrepancy is most likely due to the model dependency of the method used in this report. The MIST models used have an imperfect alignment with the red clump in the CMD and also appear to underestimate the distance to the cluster. The dominant unreliability in the isochrone-fitting method is the lack of understanding of the physical processes governing the evolution of stars. Therefore, these results highlight a persistent problem in astronomy and provide further incentive for improving stellar physics models.
The reddening measurement of E(B-V) equal to 0.30 is somewhat consistent with existing literature within an uncertainty of 0.02 – in other words, one σ from the 0.28 and 0.32 results from Burbidge & Sandage (1958) and Strom & Strom (1970) respectively. Bartašiutė & Tautvaišienė (2004) derived a result of 0.25 for the reddening which lies 2.5σ from the 0.30 obtained here. This deviation may be due to the difference in photometric systems, with the Vilnius system being used in the 2004 study.

7 CONCLUSION

This study utilised isochrone fitting and photometric analysis to estimate the age, distance, and extinction of NGC 7789. The age measurement, approximated at 1.5Gyr, was very consistent with past evaluations. The derived distance of 1800pc aligned well with other model-dependent measurements but less well with parallax measurements, emphasizing the need to reconcile model-based approaches with direct measurements. Extinction was estimated at 0.92 magnitudes, corresponding to a reddening, E(B-V), of 0.30 which was somewhat consistent with previous measurements. Identified limitations of saturation issues and uncertainties in zeropoint calculations underscore the challenges in astronomical observations with ground-based equipment, especially in areas such as Sheffield with high levels of light pollution. In summary, this study highlights the ongoing need for more precise methods to determine stellar properties as well as the need for a deeper understanding of the processes governing stars and their environments.

REFERENCES

Barnes S. A., 2007, The Astrophysical Journal, 669, 1167
Bartašiutė S., Tautvaišienė G., 2004, Astrophysics and Space Science, 294, 225
Brogaard K., VandenBerg D. A., Bedin L. R., Milone A. P., Thygesen A., Grundahl F., 2017, Monthly Notices of the Royal Astronomical Society, 468, 645
Burbidge E. M., Sandage A., 1958, Astrophysical Journal, vol. 128, p. 174, 128, 174
Choi J., Dotter A., Conroy C., Cantiello M., Paxton B., Johnson B. D., 2016, ApJ, 823, 102
Dinescu D. I., Demarque P., Guenther D., Pinsonneault M., 1995, Astronomical Journal v. 109, p. 2090, 109, 2090
Gao X.-h., 2018, Publications of the Astronomical Society of the Pacific, 130, 124101
Gim M., VandenBerg D., Stetson P., Hesser J., Zurek D., 1998, Publications of the Astronomical Society of the Pacific, 110, 1318–1335
Jørgensen, B. R. Lindegren, L. 2005, A&A, 436, 127
Lebreton Y., Montalbán J., 2008, Proceedings of the International Astronomical Union, 4, 419–430
Martinez Roger C., Paez E., Castellani V., Straniero O., 1994, Astronomy and Astrophysics, Vol. 290, p. 62-68 (1994), 290, 62
Mazzei P., Pigatto L., 1988, Astronomy and Astrophysics (ISSN 0004-6361), vol. 193, no. 1-2, March 1988, p. 148-158., 193, 148
Olsen K. A. G., Hodge P. W., Mateo M., Olszewski E. W., Schommer R. A., Suntzeff N. B., Walker A. R., 1998, Monthly Notices of the Royal Astronomical Society, 300, 665
Schultz G. V., Wiemer W., 1975, A&A, 43, 133
Soderblom D. R., 2010, Annual Review of Astronomy and Astrophysics, 48, 581
Strom K., Strom S., 1970, Astrophysical Journal, vol. 162, p. 523, 162, 523
Vallenari A., Carraro G., Richichi A., 1999, Near-infrared photometry of the intermediate age open clusters IC 166 and NGC 7789 (`arXiv:astro-ph/9910445`)

This paper has been typeset from a TEX/LATEX file prepared by the author.